Comprehensive Journal of Science
Volume (10), Issue (37), (NOV. 2025)
SICST2025, www.sicst.ly
ISSN: 3014-6266

مجلة العلوم الشاملة
عدد خاص بالمؤتمر الدولي الثالث للعلوم والتقنية
المجلد (10)، العدد (37)، (نوفمبر2025)
ردمد: 3014-6266

An Investigation into Fatigue Sensor Design and Modeling

Hatem Khalifa Said
Michanical Engineering
Higher Institute of Scince
& Technology
Azizia, Libya
hattem222@yahoo.com

Ahmed El Barouni Hadyia
Michanical Engineering
Higher Institute of Scince
& Technology
Azizia, Libya
ahmed.barouni@yahoo.com

Received: 30-09-2025; Revised: 10-10-2025; Accepted: 31-10-2025; Published: 25-11-2025

Abstract

Fatigue sensors are used as Structural Health Monitoring (SHM) mechanisms to detect damage on struc- tural components before any failures occur. In this study, a U-notched fatigue sensor was designed and analyzed to predict the fatigue life before catastrophic failure occurs. The ANSYS workbench software and 7075-T6 aluminum alloy were used to model and analyze our U-notch type fatigue sensor. The sensor model consisted of four beams of 305 × 76.2 × 1.6 mm (length × width × thickness) dimensions with different fatigue U-notch radii. It was observed that fatigue life increased with an increase in the U-notch radius. However, the value of the maximum equivalent stress decreased with an increase in the notch radius. In addition, fatigue damage occurred around the U-notch radius when the U-notch radius was equal to or less than 6.4 mm.

Keywords: ANSYS software Fatigue sensor Health monitoring U-notch sensor.

1. Introduction

Material fatigue has been a recognized phenomenon for an extended period. The industrial revolution significantly heightened interest in studying fatigue, underscoring its critical importance [1]. In recent years, numerous investigations have focused on identifying and preventing fatigue damage in the structural elements of mechanical systems, transportation vehicles, and similar applications. One such area of study involves the development of fatigue sensors to monitor the structural health of these systems.

Fatigue sensors typically feature multiple parallel beams, with each beam designed to be sensitive to varying levels of fatigue, specifically tailored for fatigue failures [2]. These sensors are characterized by their straightforward designs, cost-effectiveness, and ease of attachment to structural surfaces, enabling the monitoring of accumulated fatigue. The practical utility of these sensors extends to monitoring the health status of structural components such as aircraft wings, bridges, and marine vessels, among others. Numerous structural health monitoring applications are in use globally.

Currently, most structural health monitoring (SHM) systems rely on scheduled inspections, with ongoing efforts to implement efficient automated condition-based maintenance [3,4].

Furthermore, structural health monitoring and damage identification are gaining increasing importance in engineering. SHM is defined as the application of fatigue sensors, non-destructive sensing, and analysis of structural characteristics to ascertain whether damage has occurred, pinpoint its location, estimate its severity, and assess its impact on the remaining lifespan of the structure [5]. SHM methodologies involve exciting the system with appropriate signals and subsequently observing its response. Among active SHM techniques for determining defect location, severity, and type, the Electromechanical Impedance (EMI) method evaluates structural health by measuring the mechanical impedance using piezoelectric transducers [6].

However, the notch sensitivity of a material quantifies its susceptibility to notches or geometric discontinuities. Several factors, including notch geometry, influence notch sensitivity [7]. Gokanakonda et al. introduced the concept of a dedicated fatigue monitoring sensor, providing essential design details, simulation data, and test results that conceptually validated its effectiveness. The fatigue sensor investigated by Gokanakonda offers advantages such as its ability to be positioned at a suitable distance from the critical structural location. This sensor is exposed to the same ambient conditions as the structure itself [8]. Wang et al. provided a concise overview of eight existing fatigue damage sensors developed for detecting early fatigue damage in structures and proposed a novel approach utilizing carbon films as a fatigue monitoring sensor [9]. Additionally, Liu et al. numerically investigated the fatigue life prediction of U−notched polymethyl methacrylate (PMMA) plates by combining fatigue damage mechanisms and fatigue crack propagation mechanisms using ABAQUS. The total fatigue life of the notched plate was determined by integrating the crack initiation life with the crack propagation life [10].

The primary objective of this research is to design, analyze, and evaluate the fatigue life of a U−notch sensor for detecting fatigue failures in aircraft structural components, such as wings, as previous studies have not extensively considered this specific application. Many existing studies have concentrated on bridge structural parts, often using steel as the material. In this study, we employ a sensor with four beams, each featuring a different U−notch radius, and utilize 7075 aluminum alloy as the wing material. ANSYS workbench software is used to determine the sensor's fatigue life, providing valuable information to engineers.

2. Materials and methods

This study focuses on the design, implementation, and analysis of the sensor's fatigue life through simulation using ANSYS workbench software. The sensor model comprises four beams with a U-notch geometry, aligned parallel to the applied tension load on the structure. The fatigue sensor, specifically designed for this research, had all its dimensions precisely measured. Table 1 and Fig. 1 illustrate the magnitudes for width, length, and thickness. Furthermore, the sensor's dimensions were chosen based on the first beam assumption, where the U-notch radius was 25.4mm (more details on this assumption are available in Ref. [11]). The remaining three beams were divided into 25% (6.4mm), 50% (12.7mm), and 75% (19mm) increments to obtain fatigue life results corresponding to these divisions.

Table 1

Dimensions of the sensor.		
Width (mm)	Length (mm)	Thickness mm)
76.2	305	1.6

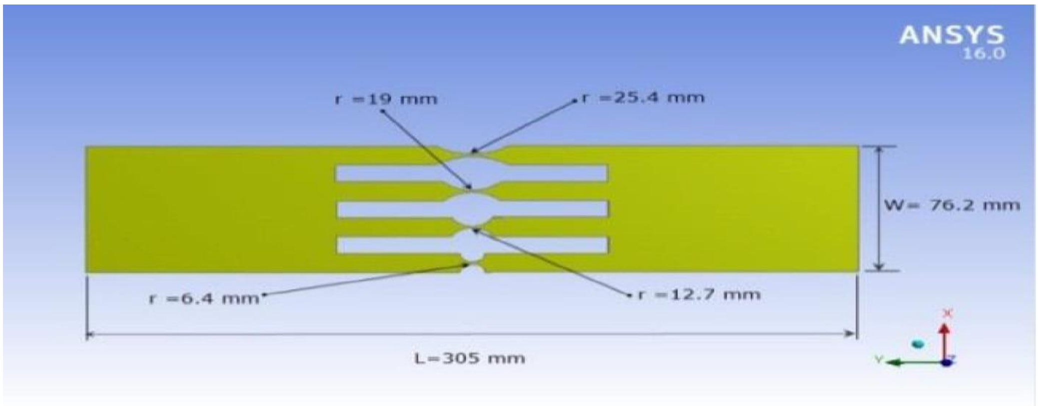

Fig. 1. Dimensions of the sensor model.

It is crucial to note that for this investigation, 7075-T6 aluminum alloy was selected due to its widespread availability and well-documented material properties. To ensure accurate simulation results by incorporating more elements in the critical U-notch region, mesh refinement became essential, as depicted in Figs. 2 and 3. Consequently, 1,212,561 mesh elements and 204,067 nodes were employed.

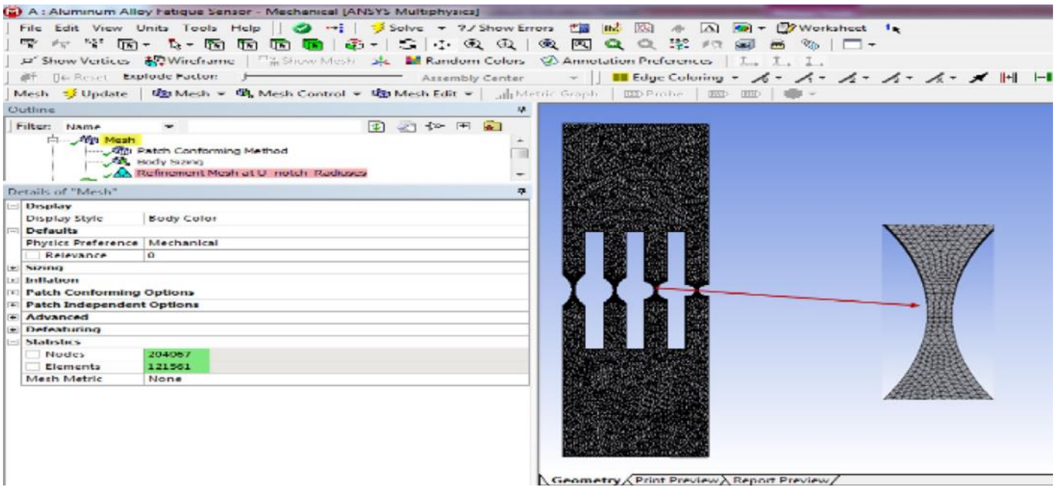

Fig. 2. Refinement mesh of the sensor model.

Fig. 3. Meshing with elements and nodes.

To confirm that stress concentration is independent of element size, a mesh sensitivity study was conducted. This study involved five different element sizes, as detailed in Table 2. Equivalent stresses were considered for the mesh sensitivity analysis. Global and/or local mesh refinement is necessary to enhance stress prediction in critical areas. The mesh sensitivity analysis was performed for the critical location (r=6.4mm) within the high-stress regions identified during the initial iterative analysis of the sensor model.

Table 2

FE model details for mesh sensitivity study.

No.	Number of Elements	Equivalent stress (MPa) (r =6.4mm)
1	11,717	93.421
2	21,095	92.023
3	39,367	91.071
4	55,222	91.023
5	121,561	90.815

Fig. 4 demonstrates the variation of equivalent stresses as a function of the number of elements. The mesh sensitivity analysis clearly indicates that the equivalent stress remains independent of the mesh size beyond 55,222 elements. Although 121,561 elements also yield identical results, they incur a higher computational cost. Since the results did not change after 121,561 elements, this refined mesh is also necessary for all subsequent analyses. Based on this finding, the stress concentration is attributed to the notch itself rather than the mesh.

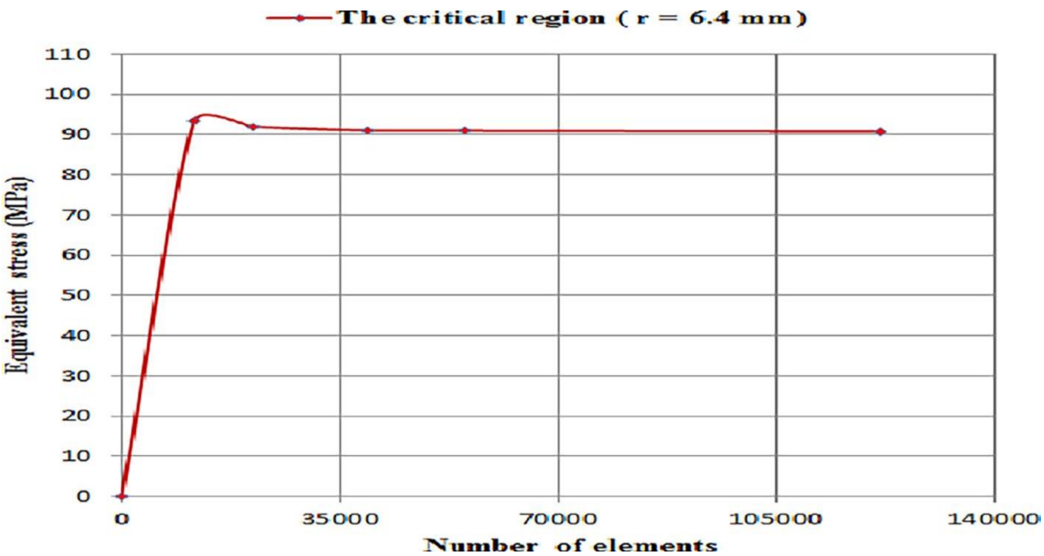

Fig. 4. Variation of equivalent stresses as a function of the number of elements.

The sensor is subjected to various applied tension loads to assess changes in the U– notch sensor's fatigue life under different loads and to optimize the high loading the sensor can withstand before failure. The magnitudes of these loads are provided in Table 3. Additionally, the sensor has a fixed boundary condition on one side, with an applied tension load on the other, as illustrated in Fig. 5.

Table 3

Magnitudes of tension loads.	
Case No.	Tension Load (N)
1	1000
2	2000
3	3000
4	4000

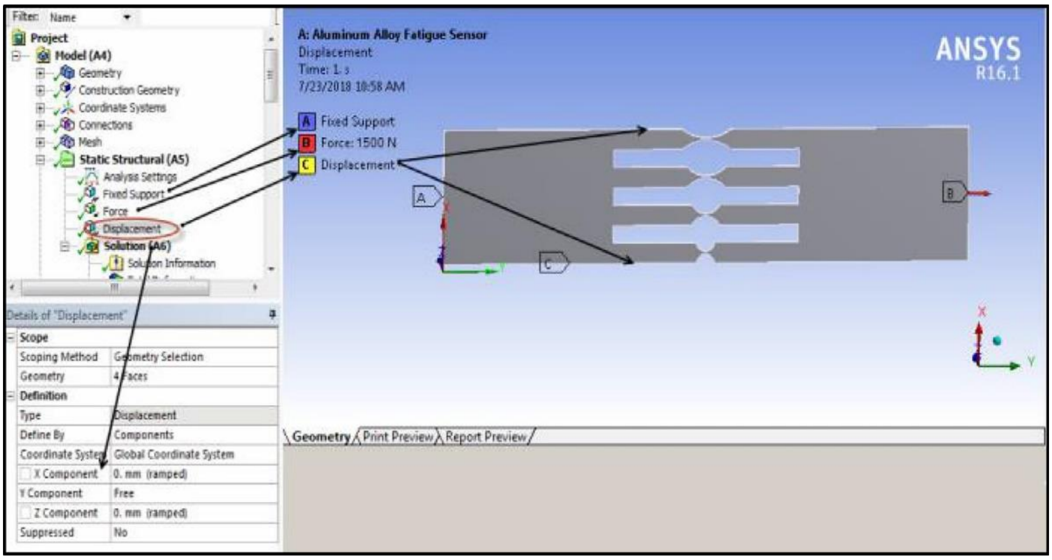

Fig. 5. Tension load and boundary conditions of the

fatigue U–notch sensor.

3. Mathematical modeling and software implementation

This section outlines the mathematical formulation of the problem and the procedure for deriving its solution. To simplify the analysis, the equations for all solution procedures are presented under the following definitions:

Stress Range:

$$r = r_{max} - r_{min} \quad (1)$$

Alternating Stress Component:

$$r = (r_{max} - r_{min})/2 \quad (2)$$

Mean Stress Component:

$$r_m = (r_{max} + r_{min})/2 \quad (3)$$

Stress Ratio:

$$R = r_{min}/r_{max} \quad (4)$$

3.1 Relationship between ultimate strength and endurance limit

The relationship between ultimate strength (Sut) and theoretical fatigue strength (Sf ′) can be defined as [12]:

$$S_{f0} = 0.4 S_{ut} \text{ for } S_{ut} < 48 kpsi (330 MPa) \quad (5.a)$$

$$S_{f0} = 19 kpsi (130 MPa) \text{ for } S_{ut} \geq 48 kpsi (330 MPa)$$

(5.b)

It is well-known that aluminum alloys do not exhibit a distinct endurance limit. Therefore, their fatigue strength (S′) is typically considered as the average failure stress at N = 5 × 108 cycles. Subsequently, the corrected fatigue strength or endurance limit (Sf) for our aluminum material model must be estimated using the following relationship:

$$S_f = C_{load} C_{size} C_{surf} C_{temp} C_{reliab} C_{miscellan} S'$$

(6)

3.2 Notch Sensitivity

Certain materials demonstrate insensitivity to notches, a characteristic often masked by the theoretical stress concentration factor. Such materials necessitate a reduced K value, denoted as Kf . In these instances, the maximum stress can be expressed as:

$$r_{max} = K_f \times r_{nor}$$

(7)

The fatigue notch factor (Kf) is defined as [13]:

$$K_f = \text{unnotched fatigue strength}/\text{notched fatigue strength}$$

(8)

Numerous methods have been proposed for calculating the fatigue notch factor. Peterson's formula for the fatigue notch factor [14], denoted as q, is given by:

$$q = (K_f - 1)/(K_t - 1)$$

(9)

Generally, the applied procedure involves first calculating Kt through geometrical

calculations of the structure. Following this, a material is selected, and its notch

sensitivity (q) for a given notch radius is determined from a chart. Subsequently,

Kf is ascertained as [15]:

$$Kf = 1 + q(Kt - 1) \quad (10)$$

When a material is subjected to stress, loading, or exhibits notch sensitivity, its capacity to withstand stress concentration requires thorough analysis. The notch sensitivity of a sample (q) is defined by specific curves and can be determined using the Khun-Hardrath formula [16].

According to Peterson's relation, the fatigue notch factor for 7075-T6 aluminum alloys is expressed as [17]:

$$Kf = 1 + (Kt - 1)/(1 + \sqrt{a}/\sqrt{r}) \quad (11)$$

where a is a material constant, and for aluminum alloy, a = 0.5mm.

3.3 S-N Curves

The fatigue properties of a material can be estimated using one or more of the following approaches:

- **Stress-life (S-N)**
- **Strain-life (e-N)**
- **Crack growth rate (da/dN-DK)**

The stress-life (S-N) curve approach is a widely used technique for determining the fatigue life of various materials. An S-N curve provides a general representation of material properties. In this context, careful consideration must be given to alternating stress and its correlation with the number of cycles to failure [18].

The S–N equation is [19]:

$$S_n = a(N)^b \quad (12)$$

where:

$$a = 0.9 S_{ut}/S_f \quad (12.a)$$

$$b = -\frac{1}{5.699}\log(0.9 S_{ut}/S_f) \quad (12.b)$$

Fig. 6 illustrates the proposed sensor modeling for fatigue life percentages. This model incorporates four distinct percentage types. In this particular model, the fourth scenario, characterized by varying fatigue life, is employed. The sensor monitors fatigue progression through the use of breakable inward fingers.

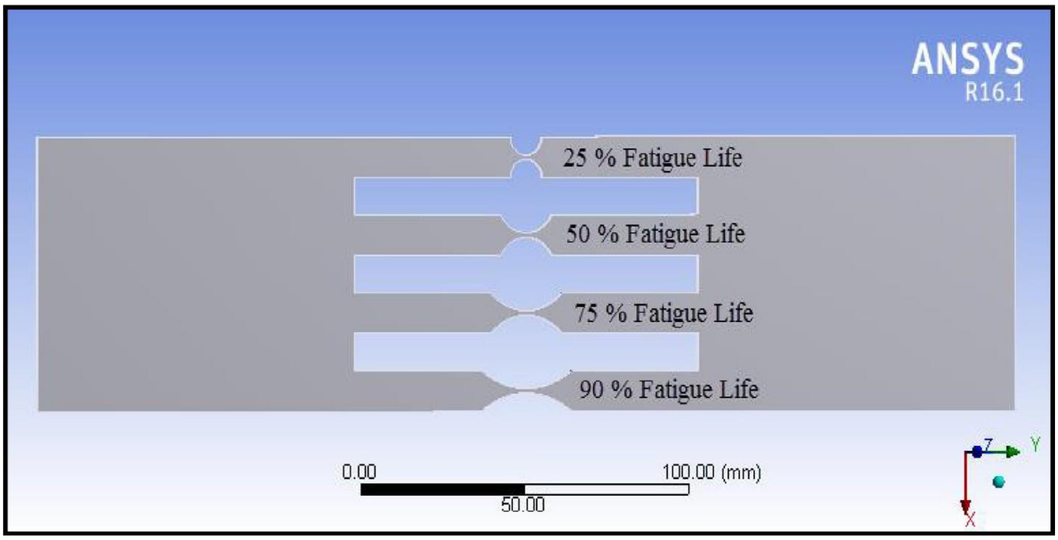

Unconventional geometrical features are utilized in the manufacturing of these inward fingers. This design ensures that the fingers will fracture upon reaching 25%, 50%, 75%, and 90% of the structure's anticipated fatigue life, thereby facilitating the monitoring of expected fatigue life without direct interaction with the sensor. Typically, a structure is replaced before it attains 90% of its projected fatigue life and prior to the occurrence of any catastrophic failure.

Fig. 6. Fatigue life percentages of the sensor.

4 Results and discussion

The primary objective of this paper is to design a fatigue sensor and utilize ANSYS simulations to estimate fatigue life, specifically employing a U-notch sensor with varying radii to mimic real structural components. This assessment was conducted using 7075-T6 aluminum alloy, whose mechanical properties, relevant to the sensor design, are detailed in Table 4.

Table 4

Mechanical properties of aluminum alloy 7075-T6 [20].	
Property	Value
Density	2.77 g/cm^3
Young's Modulus	71 GPa
Poisson's Ratio	0.33
Shear Modulus	27 GPa
Fatigue Strength (Endurance Limit)	160 MPa
Yield Strength	468.8 MPa
Ultimate Strength	579 MPa
Fatigue Strength Coefficient	887.6 Mpa
Fatigue Ductility Coefficient**	0.4664

The fatigue ductility coefficient is defined as the conventional logarithmic ductility, or monotonic fracture ductility, and is defined as:

$$ef = \ln\left(\frac{1}{1-RA}\right) \quad (13)$$

where RA represents the Reduction in Area of the test piece following a tensile test.

Table 5 presents the magnitudes of the fatigue notch factor (Kf).

The stress concentration factors (Kt) for a flat plate with opposing shallow U-notches under tension were calculated using Chart 2.6 [21]. The fatigue notch factor (Kf) can also be determined using Peterson's equation (11), as shown in Table 5.

Table 5

Magnitudes of the fatigue notch factor (K_f).

Notch Radius (mm)	Stress Concentration Factor (K_t)	Fatigue Notch Factor (K_f)
6.4	1.06	1.056
12.7	1.03	1.028
19	1.02	1.021
25.4	1.01	1.009

ANSYS simulation results indicate that the maximum directional deformation occurs along the Y-axis on the left side of the sensor (Fig. 7). This deformation exhibits symmetry between the left and right portions of the sensor. Such symmetry is a critical requirement in this context. Additionally, Figs. 8 and 9 illustrate the total deformation at the sensor's midpoint (at a length of 152.5mm). For the smallest U- notch radius (r=6.4mm), the deformation was 0.14872mm, while for the largest U- notch radius (r=25.4mm), it was 0.15166mm. This data confirms that strain varies at the notch roots due to differing notch geometries. Stress is more concentrated in these areas, making engineers particularly interested in determining the maximum stress.

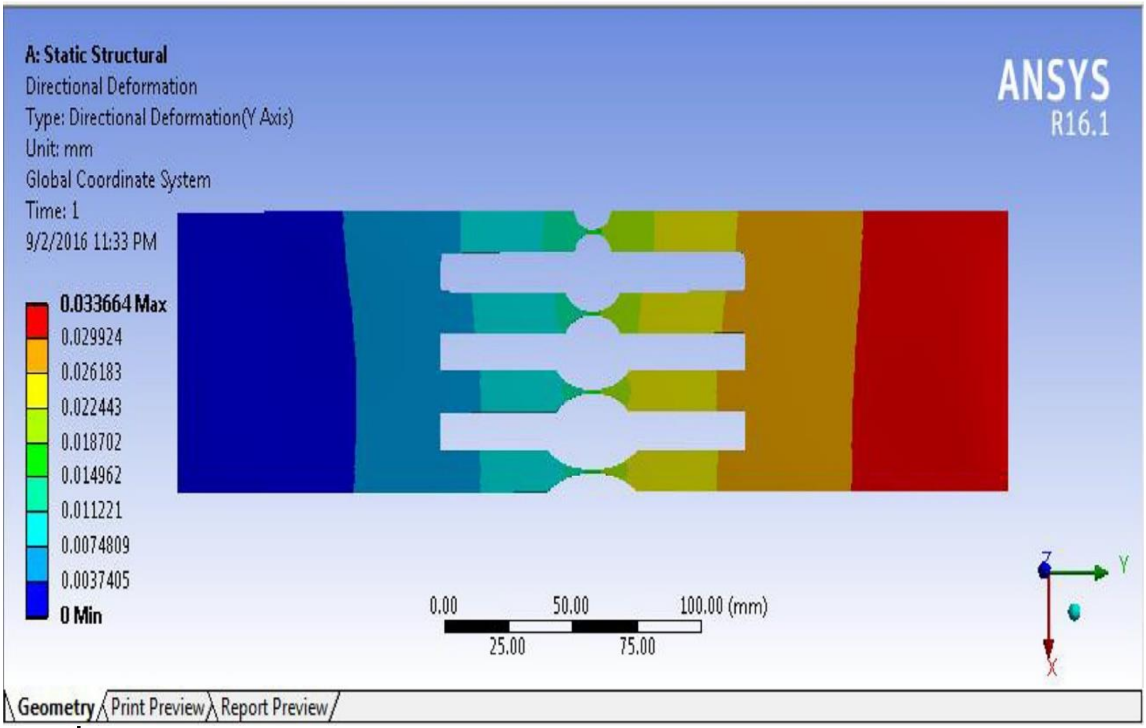

rectional deformation along the Y–axis of the sensor.

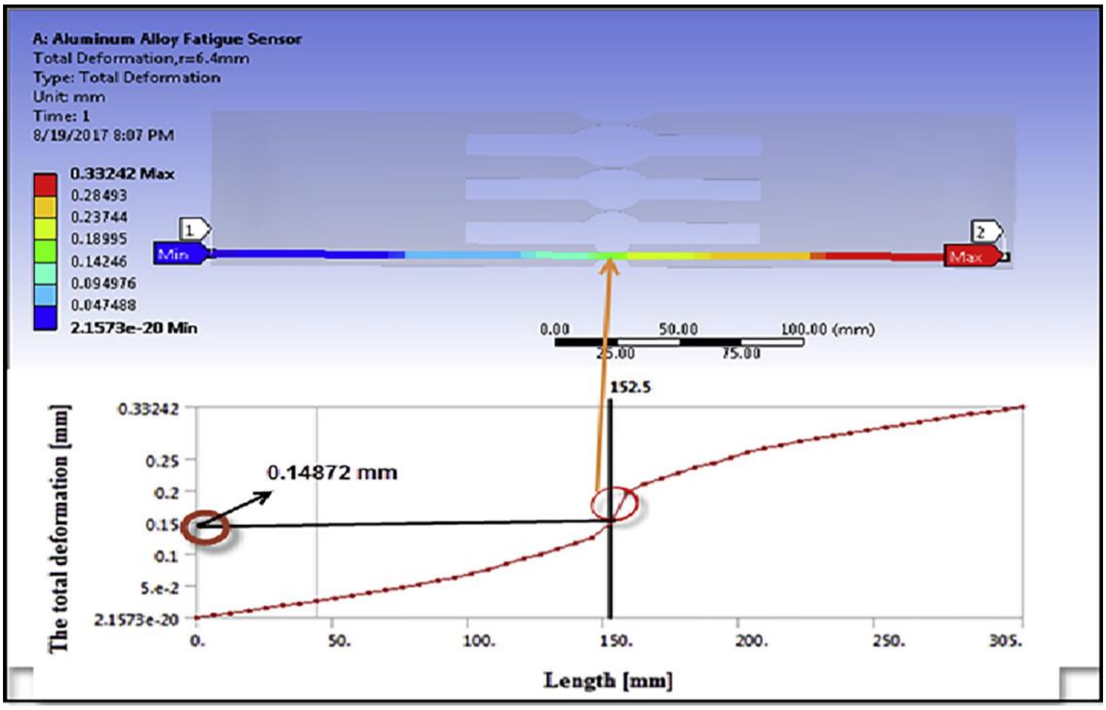

Fig. 8. Total deformation of the fatigue sensor model at r = 6.4 mm.

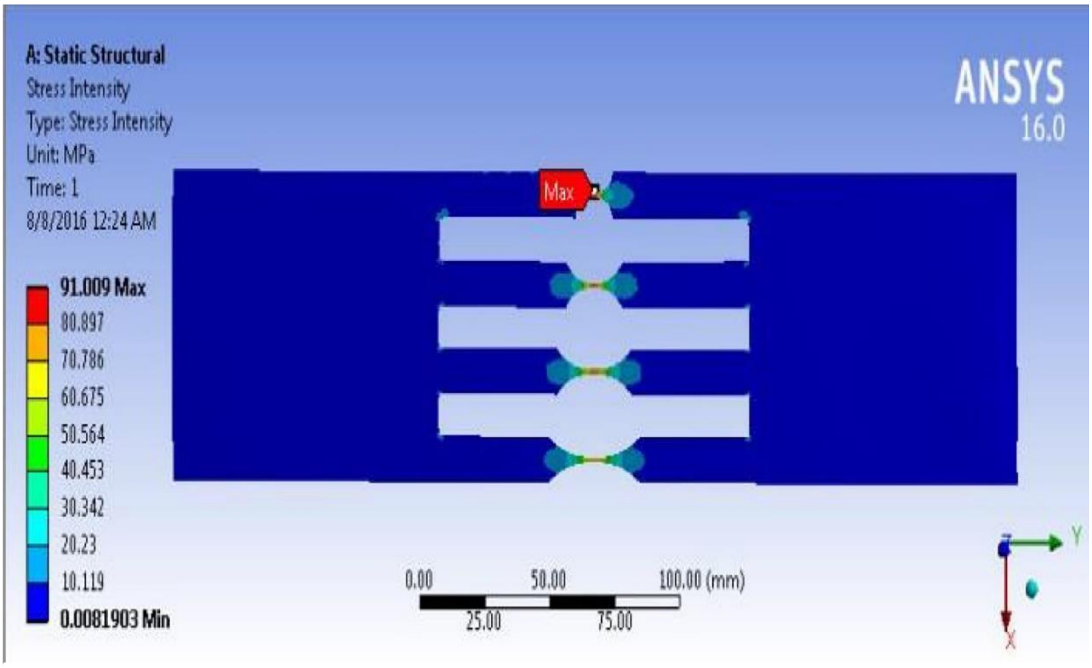

Fig. 9. Total deformation of the fatigue sensor model at r = 25.4 mm.

In reality, it is difficult to estimate the stresses at these zones. Thus, stress intensity determines whether a crack will grow or not. For this reason, Fig. 10 shows the maximum stress intensity near the U-notch geometry. The value of the maximum stress intensity at r = 6.4 mm was 91.009 MPa.

On the other hand, Fig. 11 shows the equivalent stress. Equivalent stress is part of the maximum equivalent stress failure theory used to predict yielding in a ductile material and it allows any arbitrary 2D stress state to be represented as a single positive stress value. The maximum equivalent stress value here is 90.815 MPa.

Fig. 10. Stress intensity of the sensor.

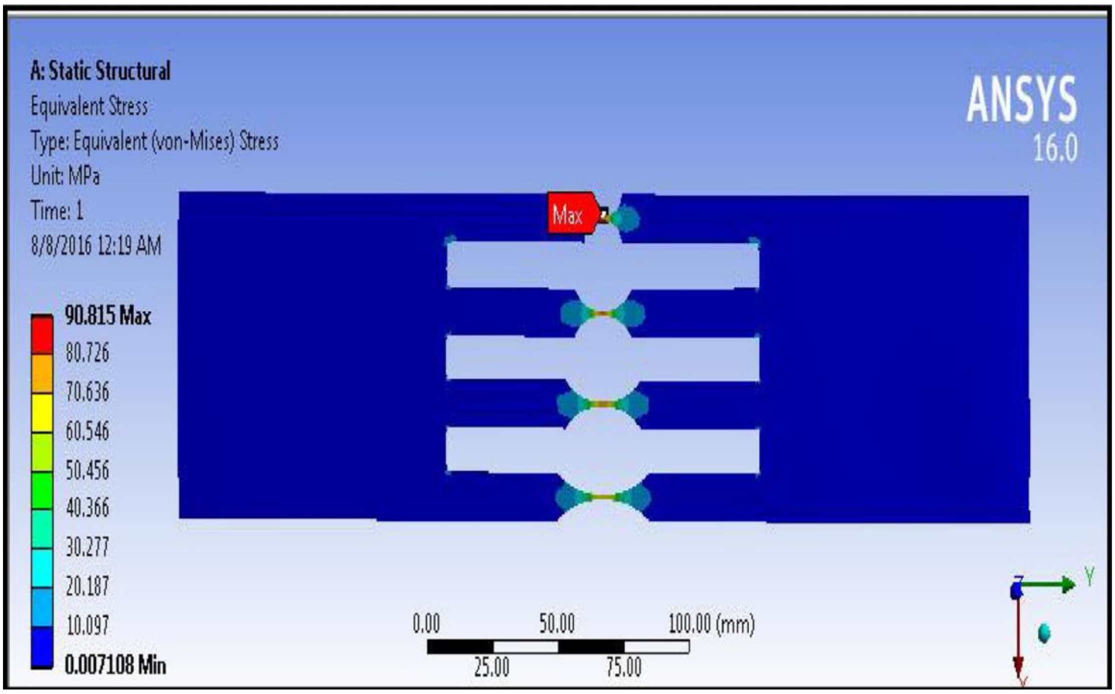

Fig. 11. Equivalent stress vs. U-notch radius.

Table 6 shows the magnitudes of the equivalent stresses achieved from the simulation results, and in order to clarify more, the results are plotted onto a graph, as in Fig. 12.

The comparison of these results with the U-notch path is illus- trated in Fig. 13. The U-notch of the small radius can fail at stresses lower than the yield stress.

J. Bannantine investigated many models of metal fatigue analy- sis and how can obtain experimental test data and transfer data into stress strain life models [22]. B. Joadder et al. studied the fail- ure cycles of round notched specimens under strain-controlled cyclic loading that were predicted using strain-life relations obtained from experiments on plain fatigue round pecimens and by using the FE model and material parameters that were validated by comparing the FE results and experimental results of LCF tests of round specimens. The value of the maximum strain was used for the prediction of failure cycles [23].

Table 6

Equivalent stress vs U-notch radius.

U-notch radius (mm)	Equivalent Stress (MPa)
6.4	90.815
12.7	78.686
19	74.41
25.4	68.715

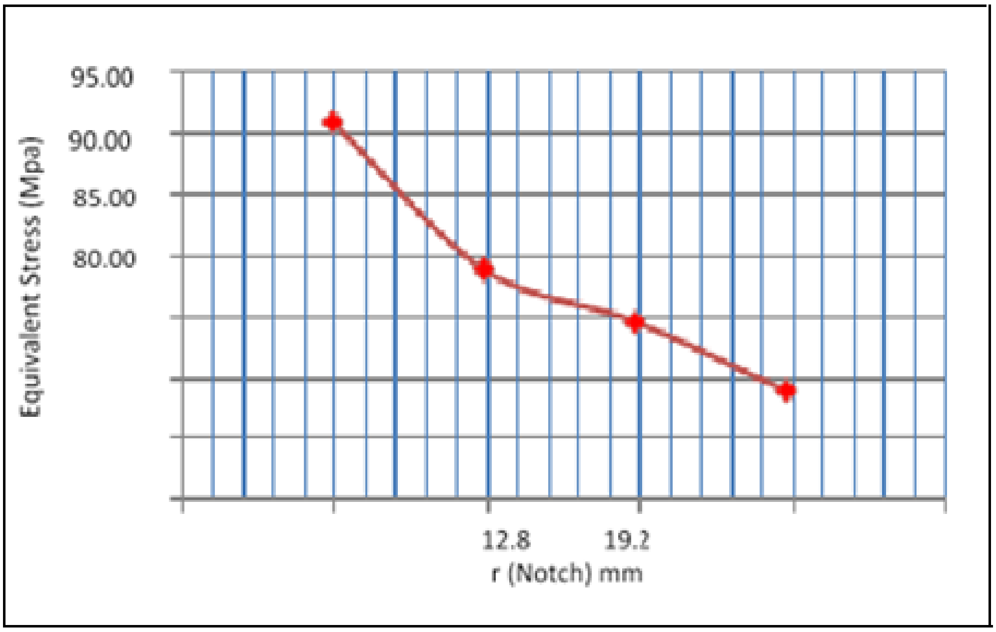

Fig. 12. Equivalent stress vs. U-notch radius.

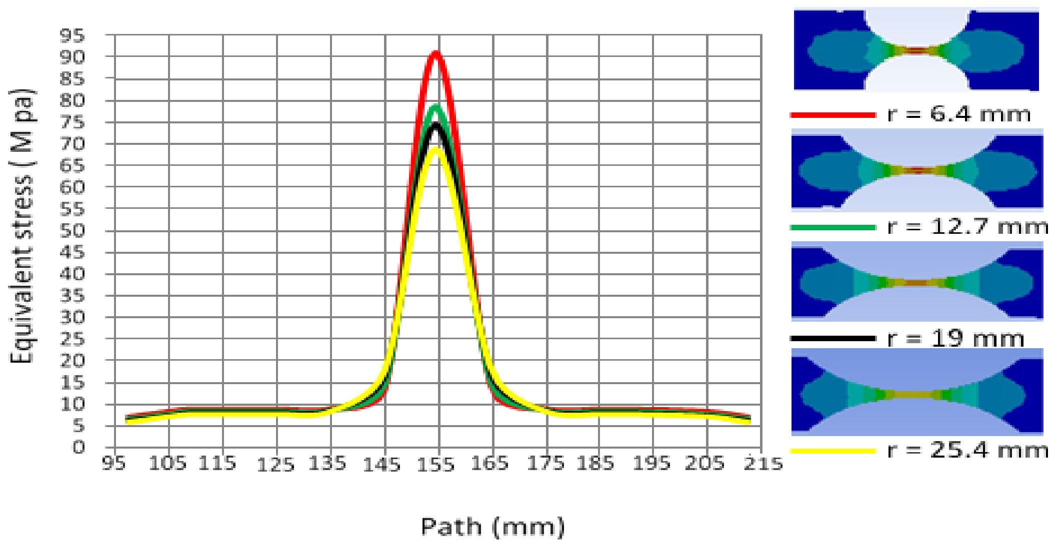

Fig. 13. Compression between equivalent stress vs. U-notch path

testing U-notched and V-notched specimens made of this material with different loading modes using the numerical method of investigation (LS-DYNA 971 software (Livermore Software Technology Corporation, Livermore, California, USA) [24]. All of these papers focused on the same purpose and support these results.

Fig. 14 shows the results that the longer fatigue life at U-notch occurred at radius r = 25.4 mm and the short fatigue life occurred at U-notch radius r = 6.4 mm because the stress concentration occurs on a smaller U-notch radius, leading first to failure. For

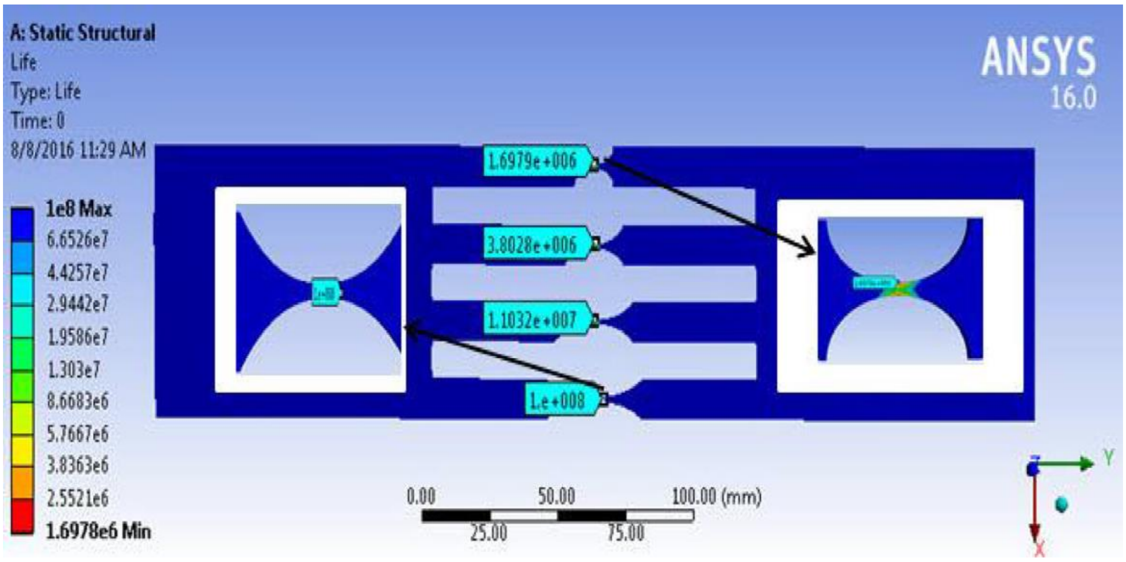

more satisfaction plotting the simulation data in the previous fig- ure to graphic shape as showed in Fig. 15, which shows fatigue life vs. U-notch radius.

Fig. 14. Fatigue life of the sensor model.

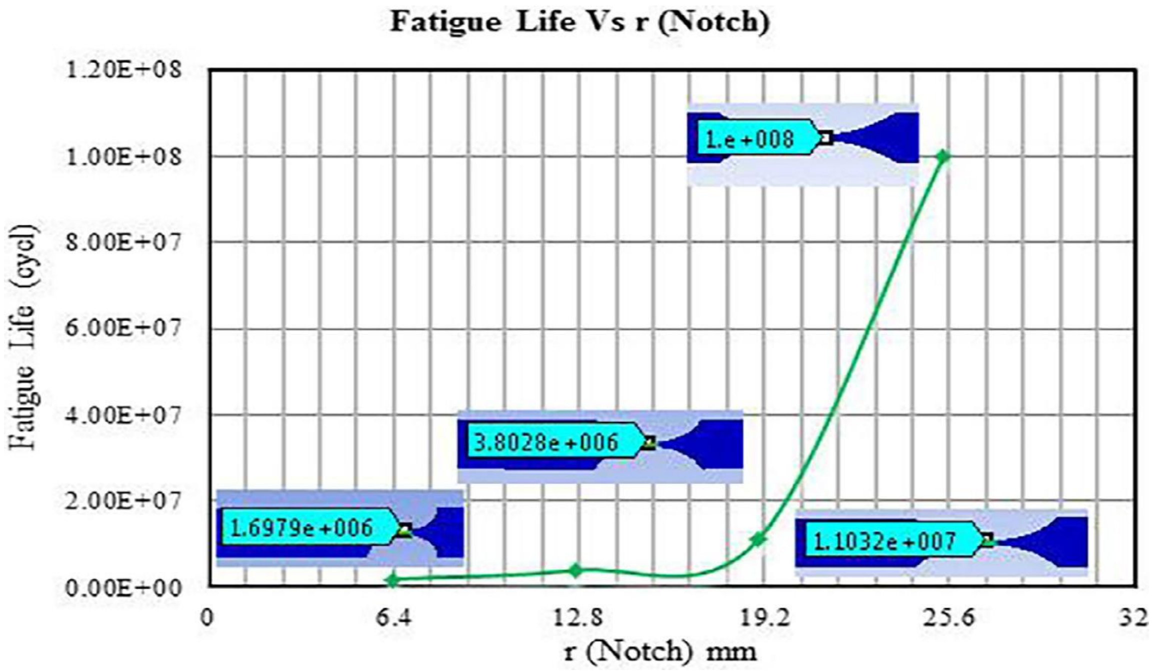

Fig. 15. Fatigue life vs. U-notch radii.

The theoretical analysis includes finding the fatigue life of the structural member using the principal stress values.

They require finding the mean stress and alternating stress to find the endur- ance limit of the structural component at particular fatigue stres- ses. The actual stress values based on measured values are given. The equations are used to calculate the fatigue life in Section 3. Therefore, the number of cycles the sensor component can with- stand before failure at maximum stress is 3.5760e+06. From Table 7, it can be observed that the theoretical fatigue life is 3.5760e+06 cycles, whereas the numerical fatigue life from soft- ware analysis is 1.6979e+06 cycles. The numerical results agree well with the theoretical results, however, the deviation between the numerical and theoretical results are comparatively apparent at the stress levels.

This is mainly because the accuracy of the pre- dicted fatigue life by simulation depends on the selection of appro- priate material model (especially mesh parameters) and the reliability of the mechanical properties of materials used [25].

Table 7

Comparison between the theoretical and numerical fatigue life of the sensor model.

Notch radius (mm)	Fatigue life (numerical)	Fatigue life (theoretical)
6.4	1.6979e+06	3.5760e+06
12.7	3.8028e+06	4.1057e+06
19	1.1032e+07	4.3092e+07
25.4	1.000e+08	4.5217e+07

Fig. 16 shows the relationship between alternating stresses and the number of cycles when using different U-notch radii as well as un-notched geometry.

The results show that a longer fatigue life was observed at U-notch radius r = 25.4 mm and a short fatigue life was observed at U-notch radius r = 6.4 mm. The stress concentration on the notch was high, which leads to failure firstly at the notch having a low fatigue life. To design a structure, characterizing the link between different factors is critical, which affects fatigue life. A popular method for this objective is characterizing this relationship using the S-N curve. Here, S represents a cyclical stress range, and N shows number cycles, after which a component or structure fails.

The notch geometry has a profound impact on the fatigue life of materials, which leads to enhancing fatigue endurance limits for every notched beam, which is part of the proposed fatigue damage sensor.

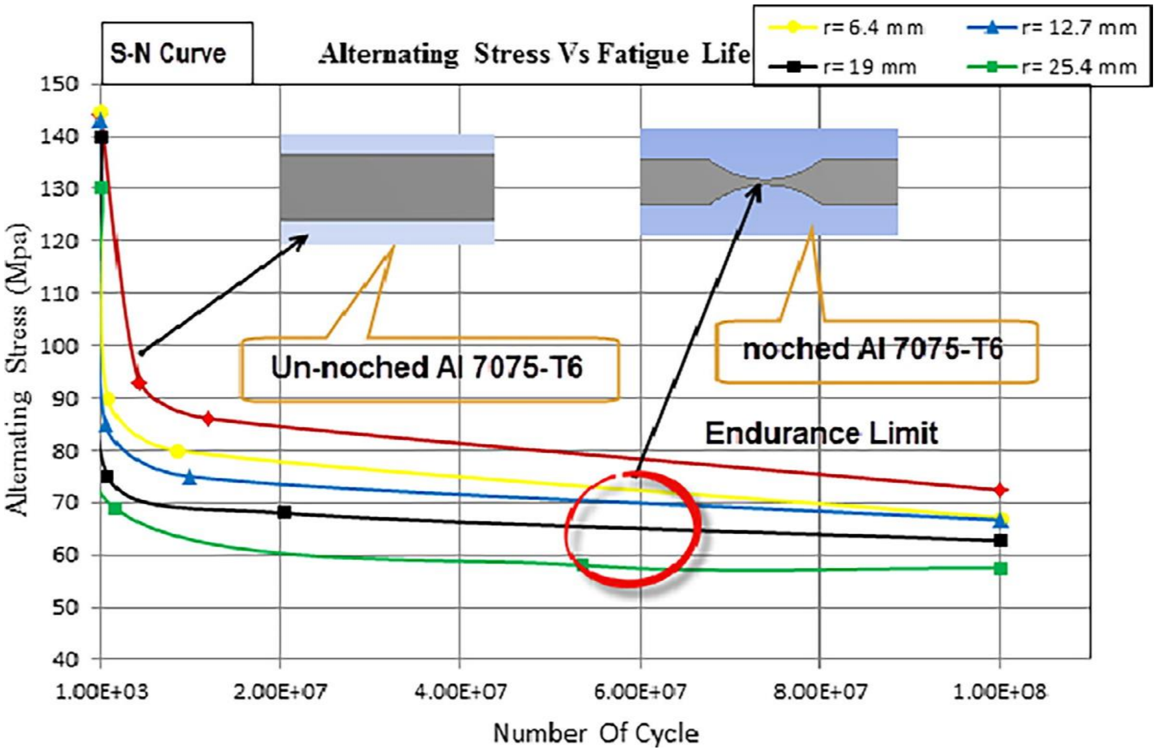

Fig. 16. Alternating stress vs. number of cycle for notched and un-notched.

5. Conclusions

The simulation of the fatigue life of U-notch fatigue sensor was modeled and the resulting simulation from the ANSYS workbench software was then used to analyze the equivalent stresses and fatigue life of different U-notch radii. The outcomes agree with the previous findings. The principal conclusions are presented as follows:

-Maximum equivalent stress decreases as notch radius increases.

-Small radii (≤6.4 mm) exhibit early fatigue damage.

–Fatigue life improves substantially with larger notches.

–Aluminum 7075-T6 beams with U-notches demonstrate reliable predictive fatigue sensing capability.

References

[1] S. Suresh, Fatigue of Materials, Cambridge University Press, 1998.

[2] T. Ozkul, H. Kaplan, M. Dolen, Wireless enabled fatigue sensor for structural health monitoring, United States Patent, 2014.

[3] S. Gokanakonda, Fabrication, Testing and Analysis of a Fatigue Sensor for Structural Health Monitoring Doctor of Philosophy, Mechanical and Aerospace Engineering, Western Michigan University, 2014.

[4] F. Chang, Structural Health Monitoring 2000, second ed., CRC Press, 1999.

[5] C. Sikorsky, Development of a health monitoring system for civil structures using a level IV non-destructive damage evaluation method, in: Proc., the 2nd International Workshop on Structural Health Monitoring, 1999, pp. 68–81.

[6] S. Tashakori, A. Baghalian, J. Cuervo, V.Y. Senyurek, I.N. Tansel, B. Uragun, Inspection of the machined features created at the embedded sensor aluminum plates, in: 2017 8th International Conference on Recent Advances in Space Technologies (RAST), 2017, pp. 517–522.

[7] G. Majzoobi, N. Daemi, The effects of notch geometry on fatigue life using notch sensitivity factor, Trans. Indian Inst. Metals 63 (2010) 547–552.

[8] S. Gokanakonda, M. Ghantasala, D. Kujawski, Fatigue sensor for structural health monitoring: design, fabrication and experimental testing of a prototype sensor, Struct. Control Health Monitor. 23 (2016) 237–251.P. Wang, T. Takagi, T. Takeno, H. Miki, Early fatigue damage detecting sensors— a review and prospects, Sens. Actuat. A: Phys. 198 (2013) 46–60.

[9] W. Liu, X. Yao, Y. Ma, X. Chen, G. Guo, L. Ma, Prediction on fatigue life of U- notched PMMA plate, Fatigue Fract. Eng. Mater. Struct. 40 (2017) 300–312.

[10] G. Pluvinage, Notch effects in fatigue and fracture, in: Notch Effects in Fatigue and Fracture, Springer, 2001, pp. 1–22.

[11] R.L. Norton, Machine design: an integrated approach, 1996, Prentice-Hall Inc, NJ, USA, 1996.

[12] B. Atzori, G. Meneghetti, M. Ricotta, Fatigue and notch mechanics, in: Applied Mechanics, Behavior of Materials, and Engineering Systems, Springer, 2017,

pp. 9–23.

[13] R. Peterson, Notch sensitivity, Metal Fatigue (1959) 293–306.

[14] W. Yao, K. Xia, Y. Gu, On the fatigue notch factor(Kf), Int. J. Fatigue 17 (1995) 245–251.

[15] P. Kuhn, H. Hardrath, An engineering method for estimating notch-size effect in fatigue tests on steel, United States Patent, 1952.

[16] R. Peterson, Stress Concentration Factors, John Wiley & Sons, New York, 1974. Google

Scholar.

[17] S. Panda, Fatigue Life Estimation of Pre-corroded 7075 Aluminium Alloy, Bachelor of Technology, National Institute of Technology, Rourkela, 2012.

[18] J. Collins, H. Busby, G. Staab, Mechanical Design of Machine Elements and Machines: A Failure Prevention Perspective, second ed., John Wiley & Sons, 2010.

[19] J. Kaufman, Introduction to Aluminum Alloys and Tempers, second ed., ASM International, United States of America, 2000.

[20] W. Pilkey, D. Pilkey, Peterson's Stress Concentration Factors, third ed., John Wiley & Sons, 2008.

[21] J. Bannantine, in: Fundamentals of Metal Fatigue Analysis, Prentice Hall, 1990, p. 273.

[22] B. Joadder, J. Shit, S. Acharyya, S. Dhar, Fatigue failure of notched specimen—a strain-life approach, Mater. Sci. Appl. 2 (2011) 1730.

[23] D. Cendon, A. Torabi, M. Elices, Fracture assessment of graphite V-notched and U-notched specimens by using the cohesive crack model, Fatigue Fract. Eng. Mater. Struct. 38 (2015) 563–573.

[24] Q. Bader, E.K. Njim, Experimental and Numerical study of influence the loading mode on Fatigue Life in Notched Steel Beam, Int. J. Sci. Eng. Res. 5 (2014).

[25] H. Kaplan, T. Ozkul, A novel smart fatigue damage sensor for structural health monitoring of critical

components of structures, in: 2016 International Conference on Industrial Informatics and Computer Systems (CIICS), 2016, pp. 1–5.

[26] R. Branco, P. Prates, J. Costa, F. Berto, A. Kotousov, New methodology of fatigue life evaluation for multiaxially loaded notched components based on two